Frontiers in Environmental Research
ISSN: 2960-026X
DOI: https://doi.org/10.61784/fer3027

CO-PYROLYSIS OF BIOMASS-BASED FURAN AND METHANOL TO LIGHT AROMATICS OVER MODIFIED HIERARCHICAL ZEOLITES

Qing Xu[1], JunMing Liang[1,2,3], DongYan Zhang[2,3], ShengPeng Xia[2,3], AnQing Zheng[2,3*], Kun Zhao[2,3], ZengLi Zhao[2,3]
[1]School of Mechanical Engineering, Guangdong Ocean University, Zhanjiang 524088, Guangdong, China.
[2]Guangzhou Institute of Energy Conversion, Chinese Academy of Sciences, Guangzhou 510640, Guangdong, China.
[3]Guangdong Provincial Key Laboratory of High-Quality Recycling of End-of-Life New Energy Devices, Guangzhou 510640, Guangdong, China.
Corresponding Author: AnQing Zheng, Email: zhengaq@ms.giec.ac.cn

Abstract: Light aromatics, including benzene, toluene, and xylene, are essential chemical feedstocks, traditionally produced via catalytic reforming of petroleum fractions. Due to the depletion of fossil resources, lignocellulose has attracted considerable interest as a renewable carbon source. Furans as key platform molecules can be catalyzed into aromatics over zeolites; however, their application is often limited by low selectivity and catalyst deactivation from coke. In this work, a co-pyrolysis approach using 2-methylfuran and methanol was developed to enhance aromatic production. Methanol served both as a heat-releasing agent during the aromatization process and as a hydrogen donor due to its high effective hydrogen-to-carbon ratio, promoting a synergistic effect with furan compounds, enhancing aromatization efficiency. Hierarchical HZSM-5 modified with Ga, Zn, Mo, and W were synthesized and characterized using various characterization techniques to correlate pore structure and acidity with product distribution. It is found that W-modified HZSM-5 can further improve the carbon yield of aromatics (70.62%), while other metal modifications resulted in decreased performance due to reduced acidity and pore blockage, accompanied by increased coke formation. This strategy provides new insight into the efficient catalytic conversion of biomass-derived platform molecules into high-value aromatics.

Keywords: 2-Methylfuran; Methanol; Zeolite; Co-pyrolysis; Light aromatic

1 INTRODUCTION

In the context of achieving carbon peaking and carbon neutrality goals, the depletion of fossil fuels and escalating environmental concerns have garnered increasing global attention. As a result, the search for clean and renewable energy sources has become a major research focus[1]. Biomass, with its capacity to be converted into high-value chemicals (e.g., sugars, fragrances, and aromatics) and liquid biofuels (e.g., biodiesel and ethanol), is widely regarded as one of the most promising clean energy sources and a key resource for realizing dual-carbon objectives.

Catalytic pyrolysis of biomass enables enhanced feedstock conversion, selective product formation, and targeted yield improvements through the action of catalysts. Catalysts can promote specific structural transformations during biomass pyrolysis, such as C-O bond cleavage or the removal of functional groups (e.g., hydroxyl, alkyl), thereby directing the reaction toward the formation of desired products and enhancing their yiedl[2-8].

Light aromatics are in high and growing demand worldwide, with the global consumption of benzene expected to exceed 107 million tonnes by 2035. Extensive research has demonstrated that co-pyrolysis of furan and olefins (such as ethylene and propylene) facilitates aromatization via the Diels–Alder (DA) reaction[9]. While olefins are highly reactive under ambient conditions, alcohols (e.g., methanol and ethanol) offer comparable functionality through methanol-to-olefins (MTO) pathways[10]. Moreover, as liquids at room temperature, alcohols are more stable and easier to store. Ivo and his co-workers have shown that replacing ethylene with ethanol significantly lowers the activation barrier, enhancing both the conversion of feedstocks and selectivity of aromatic[11]. Among alcohols, methanol—an essential building block in the chemical industry—achieved an annual production of 91.82 million tonnes in China by 2024, with a growth rate of 10.4%, substantially surpassing that of ethanol. Therefore, the co-pyrolysis of methanol with biomass-derived furans presents a viable alternative approach.

Zeolites are widely used in industrial applications due to their excellent acid-catalytic activity, thermal stability, and hydrothermal resistance. Catalyst deactivation is typically caused by low diffusion coefficients that hinder mass transfer of reactants and products within the pores, leading to pore blockage. Introducing hierarchical pore structures into zeolites helps mitigate this by retaining the shape-selectivity of micropores while improving mass transport through mesopores. Transition metals such as Fe, Cu, and Ni are frequently employed to further modify catalytic behavior, as metal incorporation can significantly alter the acidity and nature of acid sites. Incorporating metals like Mo, Zn, Ga, and W into hierarchical zeolites leverages the structural advantages of hierarchical pore structures to facilitate the aromatization of biomass-derived furans with methanol via co-pyrolysis[12-14].

This study proposes a simple and effective strategy for the efficient production of light aromatics via the co-pyrolysis of biomass-derived furans. The exothermic nature of methanol aromatization helps lower the energy barrier associated with furan conversion, while methanol's high effective hydrogen-to-carbon ratio (H/C_{eff}) provides an external hydrogen source, resulting in synergistic enhancement. Coupling this with hierarchical zeolites modified by various transition metals allows for catalyst design. The influence of different metals on product distribution during co-pyrolysis is systematically investigated. A range of characterization techniques is employed to assess changes in surface area, pore structure, acid site type and distribution, and overall acidity. This work aims to elucidate the regulatory mechanisms by which metal-modified hierarchical pore structures influence pyrolysis product selectivity.

2 EXPERIMENTAL

2.1 Catalyst Synthesis

Preparation of hierarchical zeolite: Commercial HZSM-5 (Si/Al = 25) was treated with 0.3 M NaOH solution. 10 g of HZSM-5 was added to 100 ml of 0.3 M NaOH aqueous solution and stirred in a water bath at 80 °C for 1 h. After treatment, the mixture was immediately filtered using a vacuum filtration apparatus and thoroughly washed with deionized water until the filtrate reached a neutral pH. The resulting solid was dried in an oven at 105 °C for 12 h. To remove Na+ from the alkaline treatment, the solid was then ion-exchanged with 100 ml of 1 M NH4Cl solution at 80 °C for 4 h. The exchanged material was filtered, extensively washed with deionized water, and dried overnight. The dried sample was ground and calcined in a muffle furnace at 550 °C for 2 h. The resulting hierarchical zeolite was denoted as 0.3 ZSM.

Metal modification: Metal loading was carried out via excess impregnation. Appropriate amounts of metal nitrates were dissolved in 100 ml of deionized water to prepare precursor solutions with the desired concentration. Then, 10 g of 0.3 ZSM was added to the solution and stirred in a water bath at 60 °C for 8 h. The mixture was subsequently dried overnight in an oven and calcined at 550 °C for 4 h in a muffle furnace. Each metal-modified hierarchical zeolite was synthesized with a fixed metal loading of 2 wt% and denoted as M/ZSM, where M refers to the specific metal species. The resulting catalysts were pelletized, crushed, and sieved to obtain particles in the 40-60 mesh size range for use in subsequent fixed-bed experiments.

2.2 Catalyst Tests

2-methylfuran (2-MF) and methanol (MeOH) co-pyrolysis was conducted in a fixed-bed reactor. The reaction was carried out inside a quartz tube (inner diameter: 18 mm), which was fixed and heated using a tubular furnace. Before reactions, 1 g zeolite was loaded into the quartz tube. N2 was used as the purge gas at a flow rate of 120 ml/min, while Ar served as the carrier gas during the reaction at a flow rate of 60 ml/min. A syringe pump was employed to feed the liquid reactants (mixture of 2-MF:MeOH = 1:2). All reactions were performed under atmospheric pressure. Schematic diagram of reaction device is shown in Figure 1.

The detailed procedure is as follows: before the reaction, the reactor was purged with high-purity N2 at 200 ml/min to eliminate residual air from the fixed-bed system. Meanwhile, the tubular furnace was heated to the desired temperature by temperature control system. Once the target temperature was reached, Ar was introduced as the carrier gas to establish the reaction atmosphere. The mixture of 2-MF and MeOH was then introduced at a constant flow rate via the syringe pump.

The reaction products were divided into gas, liquid and solid. The liquid products were initially captured in a condenser immersed in ethanol maintained at –60 °C, and subsequently passed through a series of gas-washing bottles for further absorption and collection. All gas-washing bottles were placed in an ice-water bath to ensure a low-temperature environment. Gas productions were collected using gas sampling bags. After the reaction, the spent catalyst was recovered as the solid product. The liquid products collected from the condenser and washing bottles, then diluted to 250 ml, and stored for subsequent analysis and characterization.

2.3 Catalyst Characterization

X-ray diffraction (XRD) patterns were recorded using an X'Pert Pro MPD diffractometer to determine the crystallinity and elemental composition of the catalysts.

Ammonia-Temperature-Programmed Desorption (NH_3-TPD) was performed using to evaluate the total acidity and acid site distribution of the zeolite catalysts. NH_3 desorption was monitored by a thermal conductivity detector (TCD). The desorption was conducted by heating the sample from 90 °C to 750 °C at a rate of 10 °C/min.

N_2 adsorption-desorption analysis was conducted using an IQ-2 instrument to determine the specific surface area, total pore volume, average pore diameter, and pore size distribution. Prior to measurement, the samples were degassed. And followed by N_2 adsorption-desorption analysis under liquid N_2 conditions.

Pyridine-adsorbed Fourier-transform infrared spectroscopy (Py-FTIR) was carried out using a Nicolet IS50 spectrometer to identify and quantify Brønsted and Lewis acid sites in the zeolite. Pyridine adsorption was performed for semi-quantitative analysis, and the Brønsted-to-Lewis acid ratio (B/L) was calculated. Combined with the total acidity from NH_3-TPD results, the individual concentrations of Brønsted and Lewis acid sites were determined.

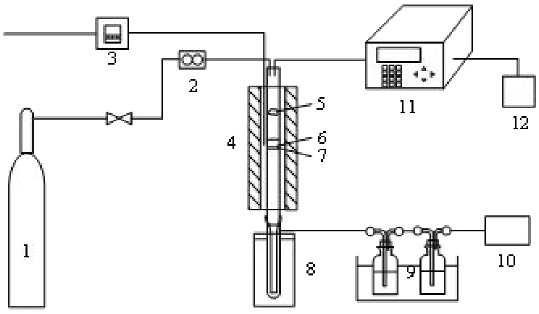

Figure 1 Schematic Diagram of Reaction Device

3 RESULTS AND ANALYSIS

3.1 Effect of Diverse Metal-Loaded Hierarchical Zeolites on Product Distribution

The specific reaction conditions were as follows: feedstock: a mixed solution of 2-MF and MeOH (molar ratio=1:2), reaction conditions: 550 °C, reaction pressure: 1 atm, WHSV: 4 h-1, carrier gas: Ar, carrier gas flow rate: 60 ml/min, reaction time: 15 min.

Figure 2 shows the mass spectra of liquid products obtained from the co-pyrolysis of 2-MF and MeOH over various metal-loaded hierarchical zeolites. As Figure 2, the distribution of products varies depending on the type of metal loaded. Nevertheless, under the pivotal role of the hierarchical pore structure all catalysts predominantly yield light aromatics, with small amounts of polycyclic aromatics also detected. The detailed retention times and identified compounds are summarized in Table 1.

As shown in Figure 3, the W-modified zeolite (W/ZSM) notably enhances the carbon yield of light aromatics (70.62%). In contrast, other metal-modified zeolites' aromatic yield decreased in different degrees. This performance deterioration can be attributed to two main factors, as supported by subsequent catalyst characterization: (i) the introduction of metal species reduces the number of acidic active sites on the catalyst surface, thereby diminishing overall acidity and catalytic efficiency; and (ii) metal oxide particles partially block the hierarchical pores, impairing mass transfer within the catalyst.

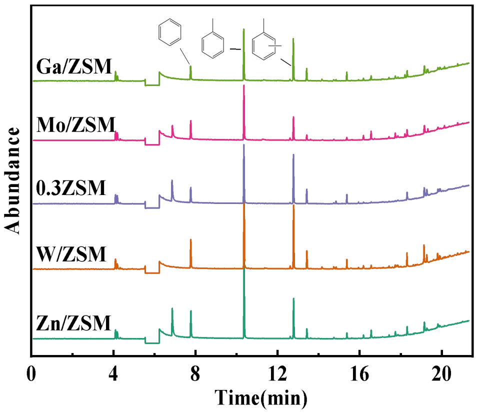

Figure 2 GC/MS Spectra of Catalytic Pyrolysis Reactions

Table 1 Main Productions of Catalytic Pyrolysis

Time	Substance
6.41	2-Methylfuran
6.88	Methoxyethane
7.77	Benzene
10.36	Toluene
12.77,12.62,13.42	Xylene
15.37	Mesitylene
16.18	Indane
16.56	indene
18.31	Naphthalene
19.15	2-Methylnaphthalene

Additionally, coke further support these findings. Compared with the unmodified hierarchical zeolite, the addition of Mo, W, or Zn significantly increases coke, with Mo/ZSM showing the highest coke of 15.61%. This excessive coke accumulation is primarily attributed tot pore blockage, which affects the mass transfer efficiency in the reaction.

Although W incorporation reduces the number of acidic active sites and partially disrupts the hierarchical pore structure, but the enhanced carbon yield of light aromatics indicates that W promotes aromatization. Moreover, both W and Ga modifications were found to suppress the formation of by-products such as methoxyethane, which is often promoted by the hierarchical pore structure. Additionally, the presence of Mo, W, and Zn appears to effectively activate C-H bonds and facilitate their cleavage, allowing residual carbon-containing fragments to recombine more freely which thereby increasing the yields of coke and polycyclic aromatics [15, 16]. This decomposition process also generates substantial amounts of low molecular weight gaseous products.

Table 2 summarizes the major gas products obtained from the co-pyrolysis of 2-MF and MeOH over different catalysts. The data clearly show that the introduction of Zn, Ga, and Mo significantly enhances hydrogen production, which is consistent with previous studies demonstrating that these metals promote the direct aromatization of methanol [17, 18]. Although direct methanol aromatization can increase aromatic yields to some extent, it bypasses the methanol-to-olefins (MTO) pathway, resulting in reduced olefin formation. This leads to limits the Diels-Alder (DA) reactions between 2-MF and olefins, ultimately reducing the overall yield of aromatics. In contrast, the W-modified zeolite facilitates the release of a larger amount of CO, thereby promoting the synergistic conversion of 2-MF and MeOH into light aromatics more effectively.

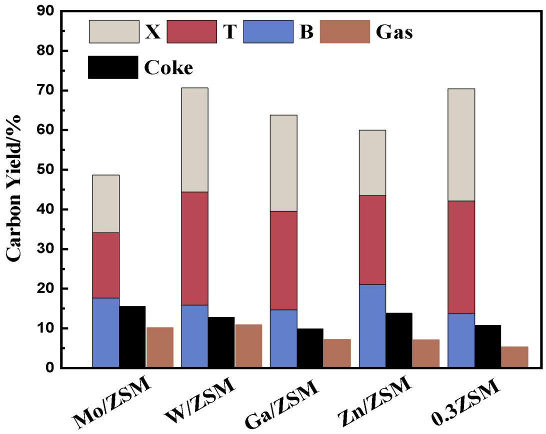

Figure 3 Carbon Yield of Different Concentration of Diverse Metal-Loaded Hierarchical Zeolites

Table 2 Gas Productions of Diverse Metal-Loaded Hierarchical Zeolites

Gas	Mo/ZSM	W/ZSM	Ga/ZSM	Zn/ZSM	0.3ZSM
CH_4	31.92%	26.24%	15.76%	11.36%	20.47%
C_2H_6	0.46%	0.77%	0.77%	0.28%	1.91%
C_2H_4	5.62%	14.14%	10.87%	4.86%	17.75%
C_3H_8	0.00%	0.28%	0.45%	0.06%	1.08%
C_3H_6	0.42%	1.35%	0.94%	0.39%	2.13%
CO_2	7.39%	5.98%	6.64%	7.87%	8.82%
CO	30.65%	41.39%	30.05%	22.28%	37.10%
H_2	23.54%	9.85%	34.53%	52.91%	12.56%

3.2 Characterization of Catalyst

The catalysts were characterized using XRD, BET, NH_3-TPD, and pyridine infrared (Py-IR) analyses.

X-ray diffraction (XRD) was employed to examine the crystallinity and elemental composition of the metal-modified hierarchical zeolites. As shown in Figure 4, all metal-loaded samples were based on the 0.3 ZSM. Characteristic diffraction peaks were observed at $2\theta = 8°$, 8.8°, 23.1°, 23.9°, and 24.4°, which are consistent with the MFI-type framework of HZSM-5. These results indicate that the incorporation of various transition metals and the presence of hierarchical pore structures did not alter the fundamental crystalline structure of the zeolite. Furthermore, the absence of distinct diffraction peaks corresponding to metal oxides suggests that the metals are either highly dispersed on the surface or incorporated into the zeolite pore channels. Combined with the results of BET, it can further prove that the metals incorporated into the channels.

N_2 adsorption-desorption isotherms were used to characterized the specific surface area, pore volume and pore size distribution of the catalysts (Figure 5). The corresponding values are summarized in Table 3. It is noteworthy that among the four metal-modified zeolites, only the Ga-loaded sample exhibited an increase in surface area and pore volume. In contrast, the other three metal-modified samples showed decreases in both parameters. Given that micropores dominate the pore structure of zeolites and contribute significantly to surface area and pore volume, the observed reductions suggest that the introduction of transition metals during impregnation leads to partial blockage of micropores. The increase observed for Ga/ZSM is likely due to Ga-induced partial recrystallization of the zeolite framework, which alters the pore structure and mitigates micropores blockage.

Figure 5a displays the N_2 adsorption-desorption isotherms for the various catalysts, all of which exhibit type IV curves with H4-type hysteresis loops, indicating the formation of mesopores and capillary condensation of micropores [19]. As shown in Figure 5b, Ga/ZSM exhibits a marked increase in mesopore volume within the 2-10 nm range, it consistent with the results of BET which further supports the role of Ga in promoting framework recrystallization and mitigating micropores blockage. In contrast, Zn-loaded zeolite significantly reduced both the mesopores (2-10 nm) and macropores (30-50 nm), suggesting severe pore blockage due to agglomeration of Zn oxides within the channels. This conclusion is corroborated by the significantly reduced surface area and pore volume listed in Table 3 for Zn/ZSM. While Mo and W also led to decreases in surface area, they resulted in increased average pore diameter, indicating that these metals mainly block micropores while leaving mesopores and macropores relatively intact, thus minimizing mass transfer limitations.

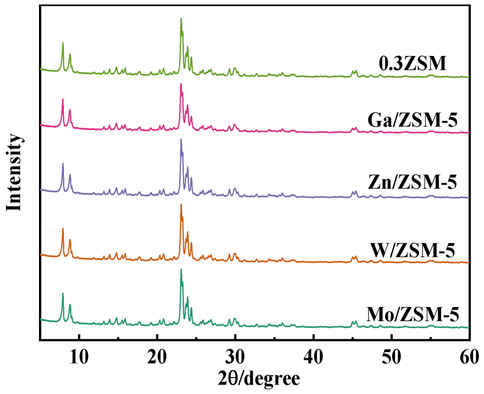

Figure 4 X-ray Diffraction Spectra of Diverse Metal-Loaded Hierarchical Zeolites

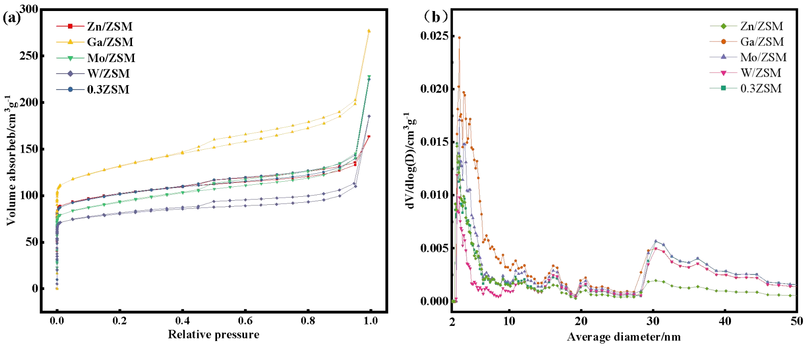

Figure 5 N_2 Adsorption and Desorption Isotherms (a) and Pore Size Analysis (b) of Diverse Metal-Loaded Hierarchical Zeolites

Table 3 Physical Properties of Diverse Metal-Loaded Hierarchical Zeolites

Catalysts	Ga/ZSM	Mo/ZSM	W/ZSM	Zn/ZSM	0.3ZSM
S_{BET}^1 (m^2/g)	481.742	343.4	308.202	384.781	379.705
V_{total}^2 (cm^3/g)	0.4288	0.3541	0.2875	0.2536	0.3489
Average Pore size^1 (nm)	3.56003	4.12443	3.73116	2.63647	3.67558

1 BET method, 2 Volume adsorbed at P/P_0=0.99

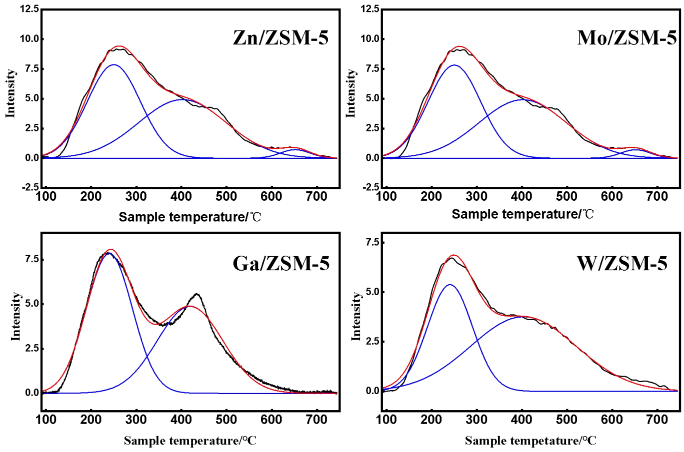

Figure 6 NH3-TPD Diagram of Diverse Metal-Loaded Hierarchical Zeolites

Table 4 NH3-TPD Results of Diverse Metal-Loaded Hierarchical Zeolites

Catalysts	First peak (°C)	Second peak (°C)	Third peak (°C)	Total acid (umol/g)
Ga/ZSM	240.21	418.97	-	1425.8
W/ZSM	240.62	403.22	-	1328.8
Zn/ZSM	250.27	401.67	651.77	1678.4
Mo/ZSM	250.16	402.10	651.80	1749.8

NH_3-temperature programmed desorption (NH_3-TPD) was employed to characterize the strength and distribution of acid sites in the catalysts (See Table 4). The acidity profiles of various metal-modified hierarchical zeolites are shown in Figure 6. Two characteristic desorption peaks were observed: one in the low-temperature region around 250 °C, typically attributed to NH_3 desorption from weak acid sites, and another in the high-temperature region near 450 °C, generally corresponding to NH_3 desorption from strong acid sites [15]. Table 5 presents the fitted curves of NH_3-TPD and the corresponding total acidity values. The data indicate that the introduction of metal oxides weakens the strength of medium-to-strong acid sites, as evidenced by the diminished intensity of the corresponding peaks. Notably, a very weak desorption peak appeared near 650 °C for Mo/ZSM and Zn/ZSM, which is typically associated with NH3 desorption from strong acid sites. This phenomenon may result from a synergistic interaction between Mo or Zn with the zeolite, leading to NH_3 desorption at elevated temperatures.

Overall, these results demonstrate that the incorporation of transition metals significantly alters both the type and number of acid sites on the catalyst. For Ga- and W-loaded samples, the total acidity was found to be lower than that of the unmodified hierarchical zeolite, suggesting that Ga and W species may have entered the pore channels of the zeolite [15].

Figure 7 shows the FTIR spectra of the zeolites measured at 200 °C. The characteristic absorption peaks at 1545, 1454, and 1490 cm-1 respectively correspond to pyridine adsorbed on Brønsted acid sites, Lewis acid sites, and the combined B+L acid sites [20].

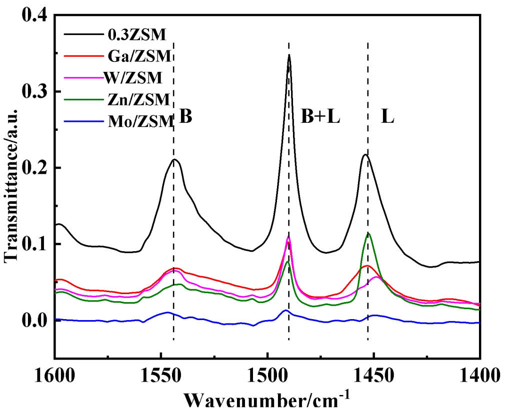

Figure 7 Py-IR Spectra of Diverse Metal-Loaded Hierarchical Zeolites

Table 5 Py-IR Acidity Distribution of Diverse Metal-Loaded Hierarchical Zeolites

Catalysts	Lewis (umol/g)	Brønsted (umol/g)	B/L	Total acid (umol/g)
0.3ZSM	635.7	896.3	1.41	1532.0
Mo/ZSM	438.0	1311.8	2.99	1749.8
Zn/ZSM	1271.2	407.2	0.33	1678.4
W/ZSM	437.5	891.3	2.04	1328.8
Ga/ZSM	684.5	741.3	1.08	1425.8

4 CONCLUSIONS

Based on the hierarchical zeolite, metal-modified catalysts were designed and applied to the co-pyrolysis of bio-based furans and methanol, resulting in a significant enhancement in aromatic yield. The results showed that tungsten (W) loading on hierarchical HZSM-5 further improved the catalytic performance, leveraging the advantages of the hierarchical pore structure, and achieved a light aromatics yield of 70.62%. In contrast, the other three metals led to a decline in overall acidity due to interactions with the acid sites of the zeolite. Moreover, partial pore blockage caused by certain metals restricted mass transfer of the reactants, thereby diminishing the catalytic activity and reducing aromatic yields.

COMPETING INTERESTS

The authors have no relevant financial or non-financial interests to disclose.

FUNDING

The National Natural Science Foundation of China (Grants 52476190, 52276221 and 22279144); Guangdong Natural Science Funds for Distinguished Young Scholar (Grants 2023B1515020093 and 2023B1515020048).

REFERENCES

[1] WANG S R, DAI G X, YANG H P, et al. Lignocellulosic biomass pyrolysis mechanism: A state-of-the-art review. Progress in Energy and Combustion Science, 2017, 62: 33-86. DOI: 10.1016/j.pecs.2017.05.004.

[2] BRIDGWATER A V. Review of fast pyrolysis of biomass and product upgrading. Biomass & Bioenergy, 2012, 38: 68-94. DOI: 10.1016/j.biombioe.2011.01.048.

[3] BUTLER E, DEVLIN G, MEIER D, et al. Fluidised bed pyrolysis of lignocellulosic biomasses and comparison of bio-oil and micropyrolyser pyrolysate by GC/MS-FID. Journal of Analytical and Applied Pyrolysis, 2013, 103: 96-101. DOI: 10.1016/j.jaap.2012.10.017.

[4] CHENG Y T, JAE J, SHI J, et al. Production of Renewable Aromatic Compounds by Catalytic Fast Pyrolysis of Lignocellulosic Biomass with Bifunctional Ga/ZSM-5 Catalysts. Angewandte Chemie-International Edition, 2012, 51(6): 1387-90. DOI: 10.1002/anie.201107390.

[5] ICHARD F, STEFAN C. Catalytic pyrolysis of biomass for biofuel production. Fuel Processing Technology, 2010, 91(1): 25-32.

[6] DHYANI V, BHASKAR T. A comprehensive review on the pyrolysis of lignocellulosic biomass. Renewable Energy, 2018, 129: 695-716. DOI: 10.1016/j.renene.2017.04.035.

[7] MISSON M, HARON R, FADHZIR M, et al. Pretreatment of empty palm fruit bunch for production of chemicals via catalytic pyrolysis. Bioresource Technology, 2009, 100(11): 2867-73. DOI: 10.1016/j.biortech.2008.12.060.

[8] SUN L Z, WANG Z B, CHEN L, et al. Catalytic Fast Pyrolysis of Biomass into Aromatic Hydrocarbons over Mo-Modified ZSM-5 Catalysts. Catalysts, 2020, 10(9). DOI: 10.3390/catal10091051.

[9] CHENG Y-T, HUBER G W. Production of targeted aromatics by using Diels–Alder classes of reactions with furans and olefins over ZSM-5. Green Chemistry, 2012, 14(11): 3114. DOI: 10.1039/c2gc35767d.

[10] RAHIMI N, KARIMZADEH R. Catalytic cracking of hydrocarbons over modified ZSM-5 zeolites to produce light olefins: A review. Applied Catalysis a-General, 2011, 398(1-2): 1-17. DOI: 10.1016/j.apcata.2011.03.009.

[11] TEIXEIRA I F, LO B T, KOSTETSKYY P, et al. From Biomass-Derived Furans to Aromatics with Ethanol over Zeolite. Angew Chem Int Ed Engl, 2016, 55(42): 13061-6. DOI: 10.1002/anie.201604108.

[12] LIU Y, LI D, WANG T, et al. Efficient Conversion of Methane to Aromatics by Coupling Methylation Reaction. ACS Catalysis, 2016, 6(8): 5366-70. DOI: 10.1021/acscatal.6b01362.

[13] SU X, ZAN W, BAI X, et al. Synthesis of microscale and nanoscale ZSM-5 zeolites: effect of particle size and acidity of Zn modified ZSM-5 zeolites on aromatization performance. Catalysis Science & Technology, 2017, 7(9): 1943-52. DOI: 10.1039/c7cy00435d.

[14] CHENG Y T, JAE J, SHI J, et al. Production of renewable aromatic compounds by catalytic fast pyrolysis of lignocellulosic biomass with bifunctional Ga/ZSM-5 catalysts. Angew Chem Int Ed Engl, 2012, 51(6): 1387-90. DOI: 10.1002/anie.201107390.

[15] ZHENG Y, WANG F, YANG X, et al. Study on aromatics production via the catalytic pyrolysis vapor upgrading of biomass using metal-loaded modified H-ZSM-5. Journal of Analytical and Applied Pyrolysis, 2017, 126: 169-79. DOI: 10.1016/j.jaap.2017.06.011.

[16] YEH Y-H, GORTE R J. Study of Zn and Ga Exchange in H-[Fe]ZSM-5 and H-[B]ZSM-5 Zeolites. Industrial & Engineering Chemistry Research, 2016, 55(50): 12795-805. DOI: 10.1021/acs.iecr.6b03659.

[17] SHEN X, KANG J, NIU W, et al. Impact of hierarchical pore structure on the catalytic performances of MFI zeolites modified by ZnO for the conversion of methanol to aromatics. Catalysis Science & Technology, 2017, 7(16): 3598-612. DOI: 10.1039/c7cy01041a.

[18] CHU S, GUO X, LI J, et al. Synthesis of Ga2O3/HZSM-5@cubic ordered mesoporous SiO2 with template Pluronic F127 to improve its catalytic performance in the aromatization of methanol. Journal of Porous Materials, 2016, 24(4): 1069-78. DOI: 10.1007/s10934-016-0347-0.

[19] SING K S W, WILLIAMS R T. Physisorption Hysteresis Loops and the Characterization of Nanoporous Materials. Adsorption Science & Technology, 2004, 22(10): 773-82. DOI: 10.1260/0263617053499032.

[20] ZHANG X, ZHONG J, WANG J W, et al. Catalytic performance and characterization of Ni-doped HZSM-5 catalysts for selective trimerization of n-butene. Fuel Processing Technology, 2009, 90(7-8): 863-70. DOI: 10.1016/j.fuproc.2009.04.011.